Supporting Information

Non-Salen Coumarin Schiff Base Chiral Fluorescent Probe Turn on Circularly Polarized Luminescence by Mg^{2+} and Zn^{2+}

Fubin Fu, Xueyan Zhang, Shengquan Zhou,Wei Shi, Jiangmin Li, Jiajia Yu, Yanzhao Rao, Lei Wu, Jing Cao*

College of Chemistry,Xiangtan University, Xiangtan City, Hunan Province, 411105, China

Email: caojing8088@xtu.edu.cn

Contents

Computational Studies. The DFT calculations were performed by using the Gaussian 09 program4 at the B3LYP 6-311(g)level.

^{1}H and ^{13}C Spectra of Compounds

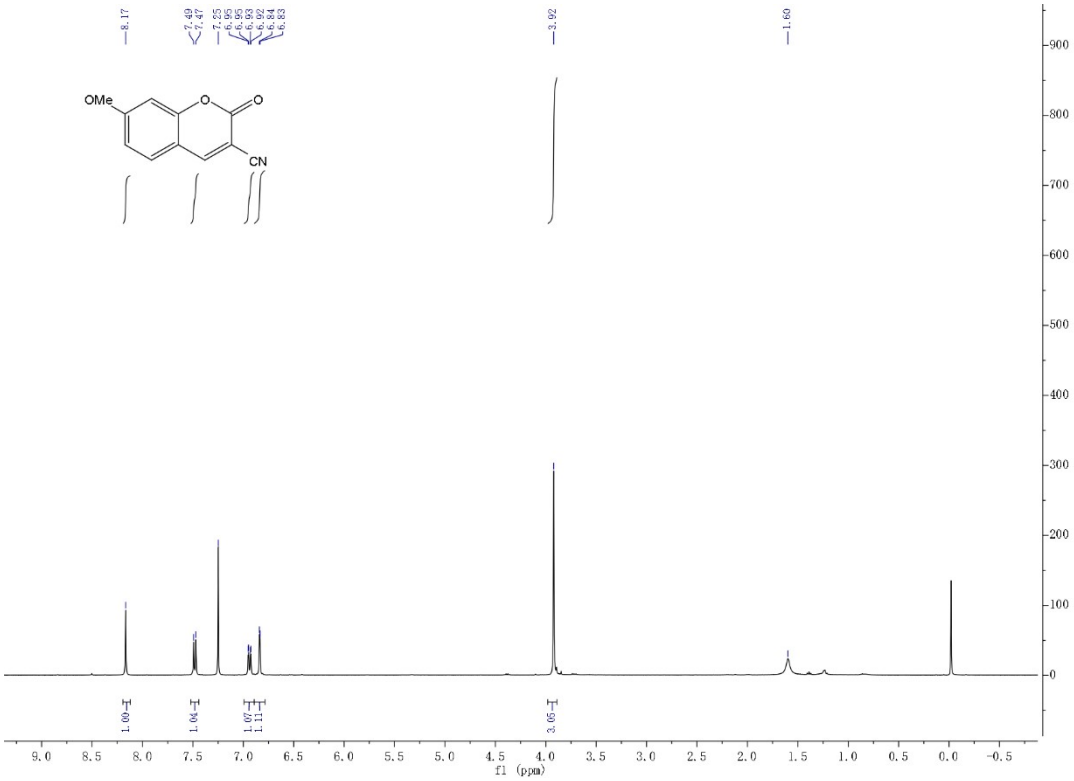

Figure S1. [1] H NMR spectrum of the compound 2a

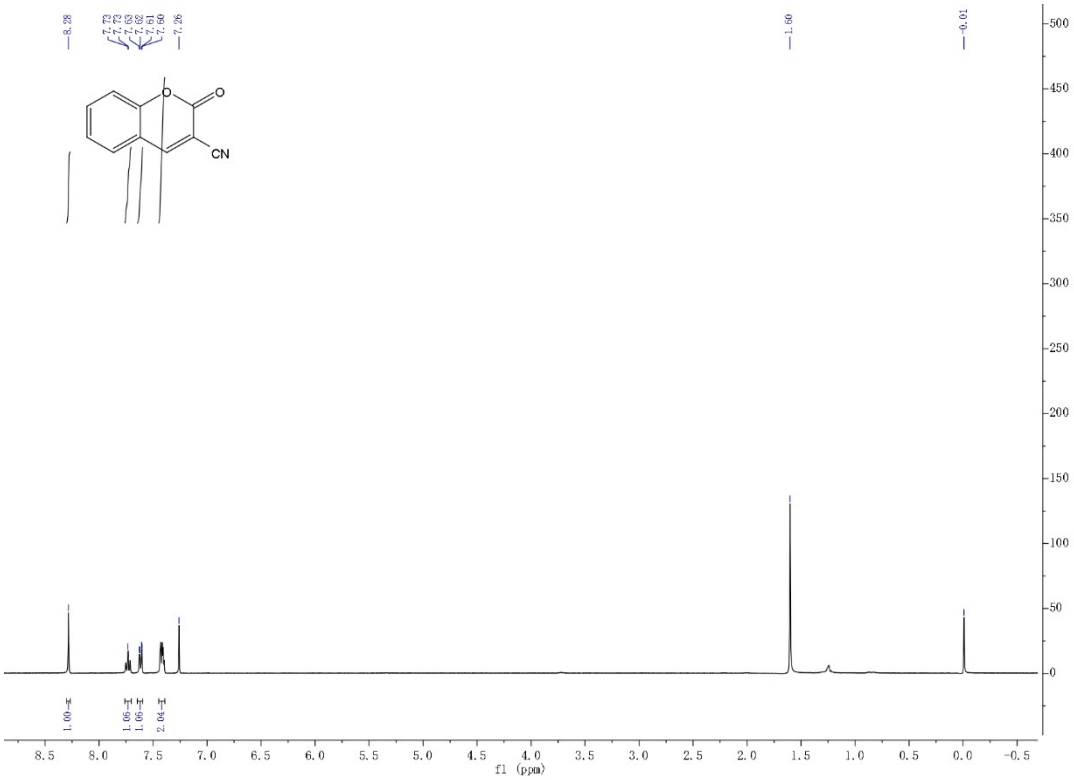

Figure S2 . [1] H NMR spectrum of the compound 2b

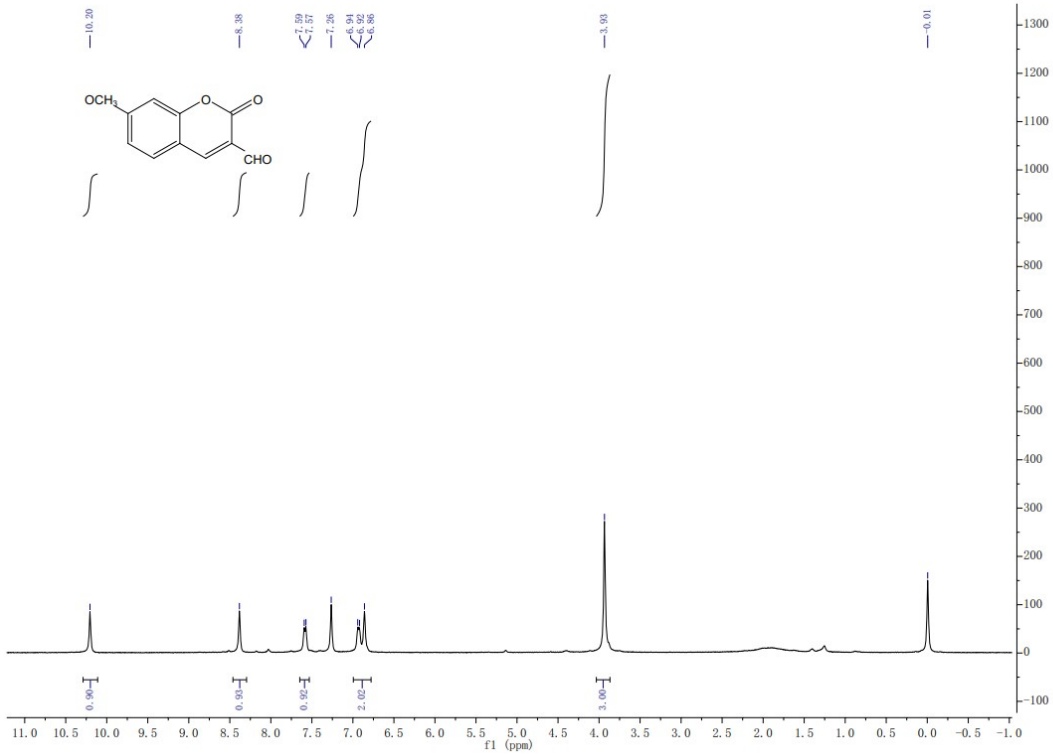

Figure S3 . [1] H NMR spectrum of the compound 3a

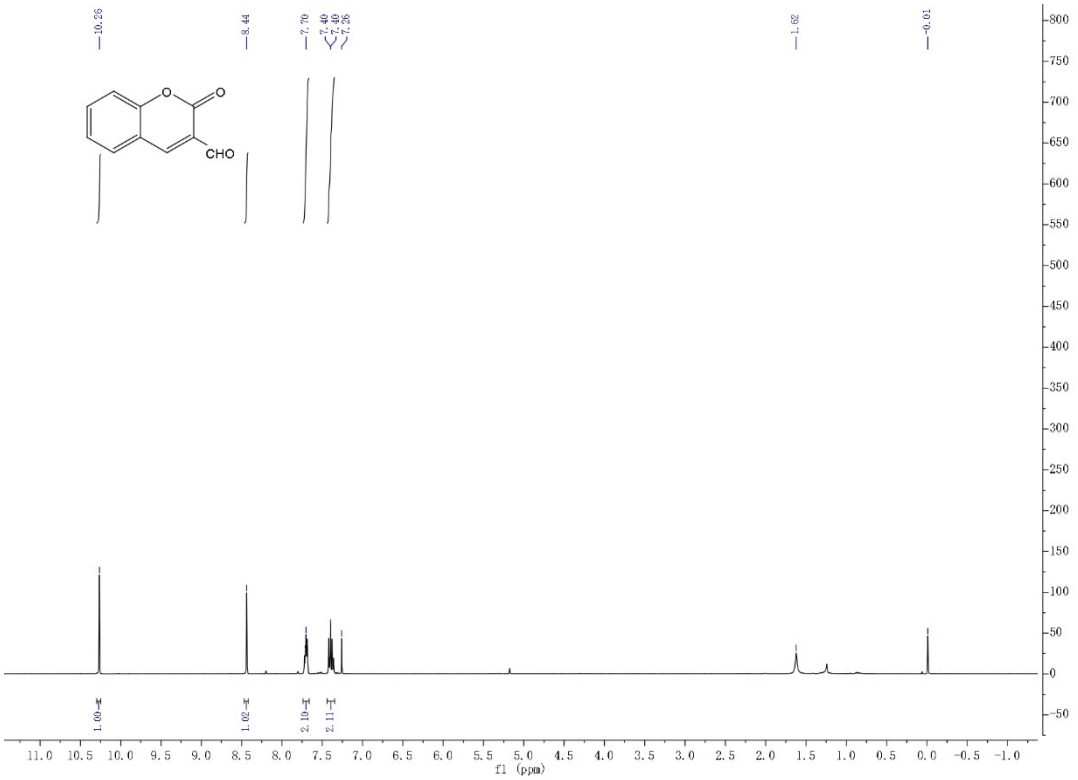

Figure S4 . [1] H NMR spectrum of the compound 3b

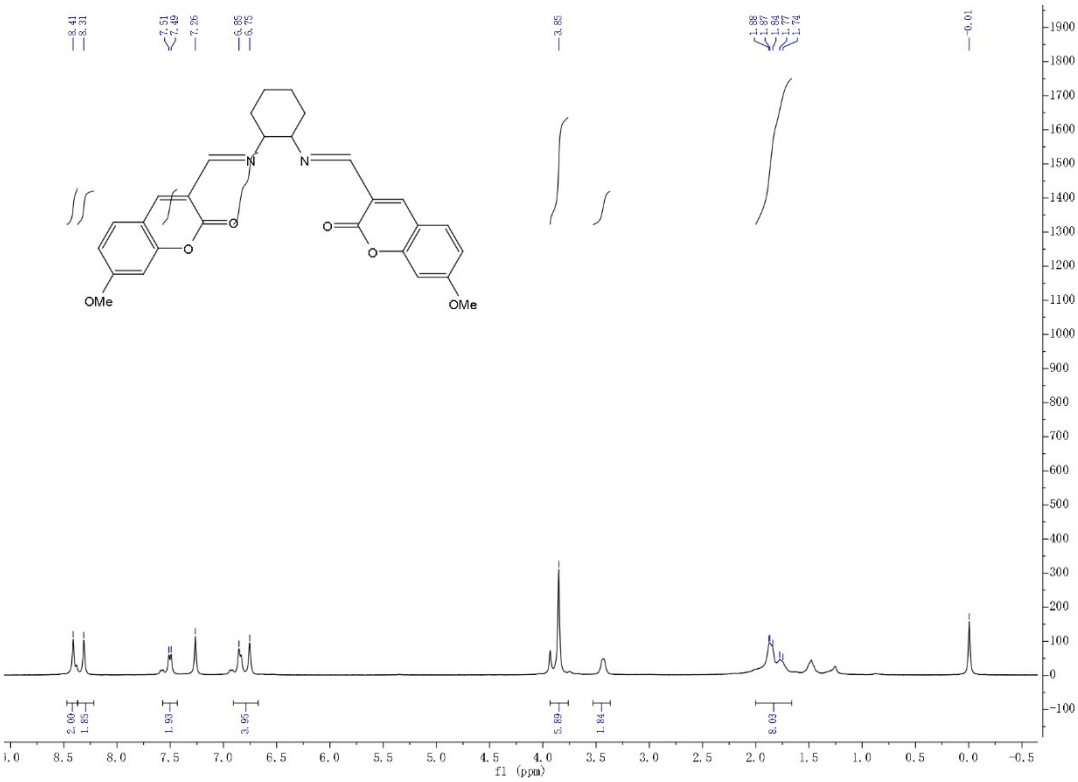

Figure S5 . [1] H NMR spectrum of the compound L1

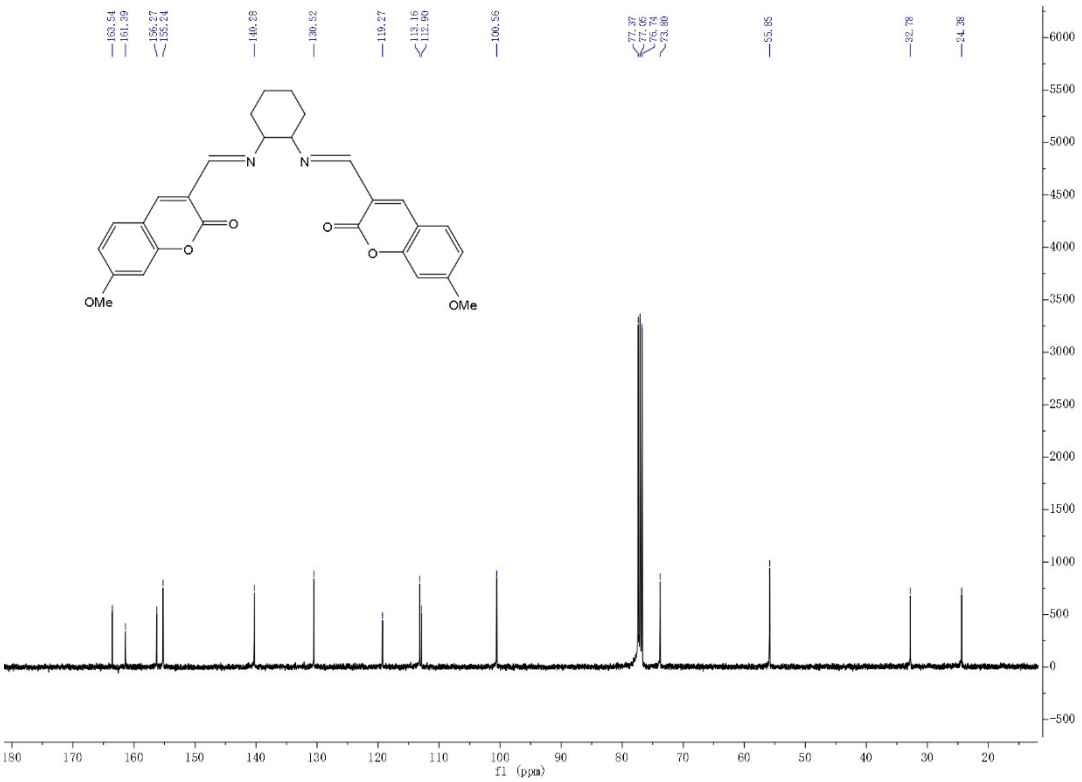

Figure S6 . [13] C NMR spectrum of the compound L1

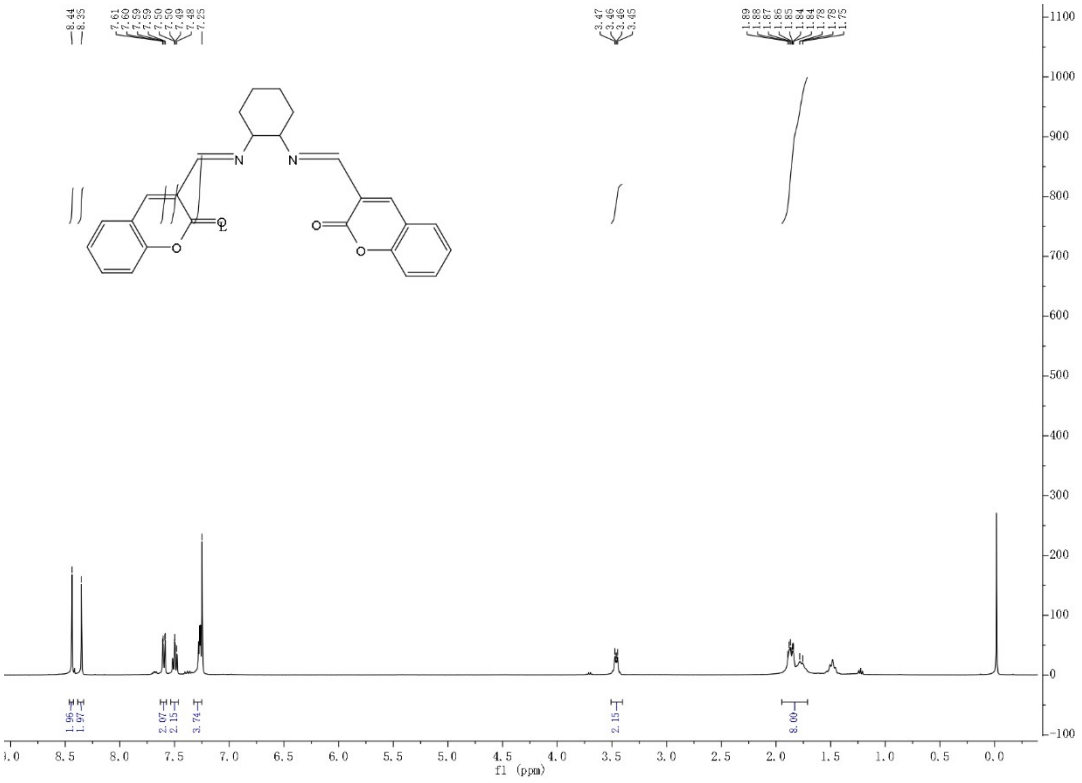

Figure S7 . [1] H NMR spectrum of the compound L2

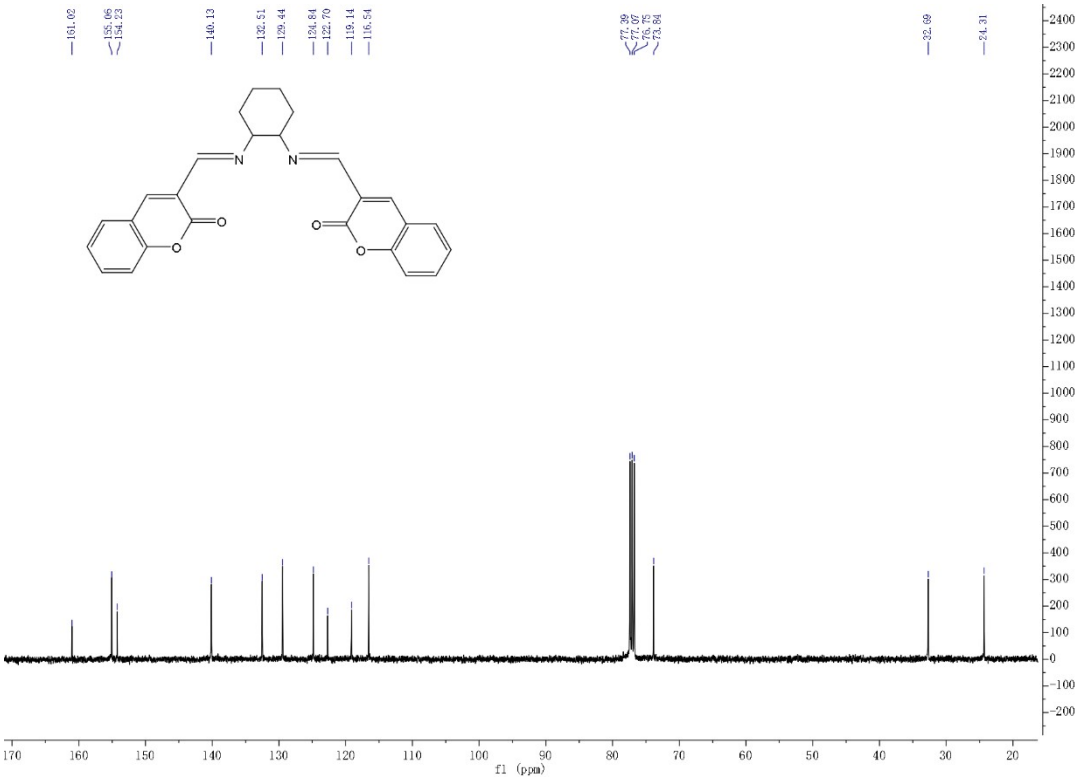

Figure S8 . ^{13} C NMR spectrum of the compound L2

LC-MS spectrum of the compound L

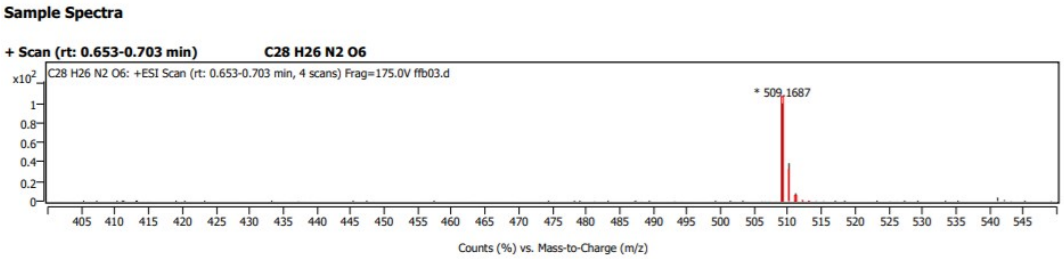

Figure S9. LC-MS spectrum of the compound L1

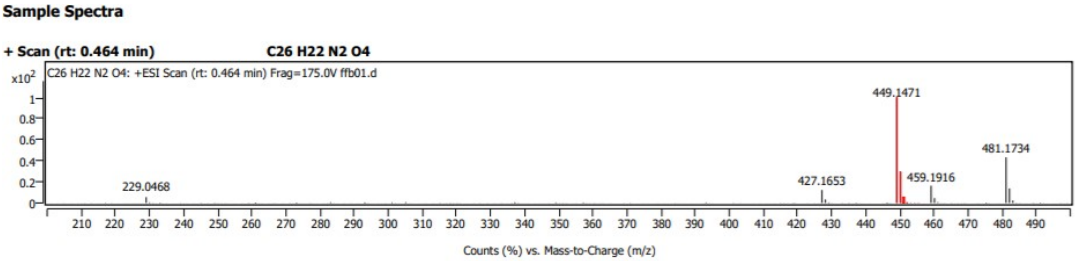

Figure S10. LC-MS spectrum of the compound L2

photophysical properties of the probe

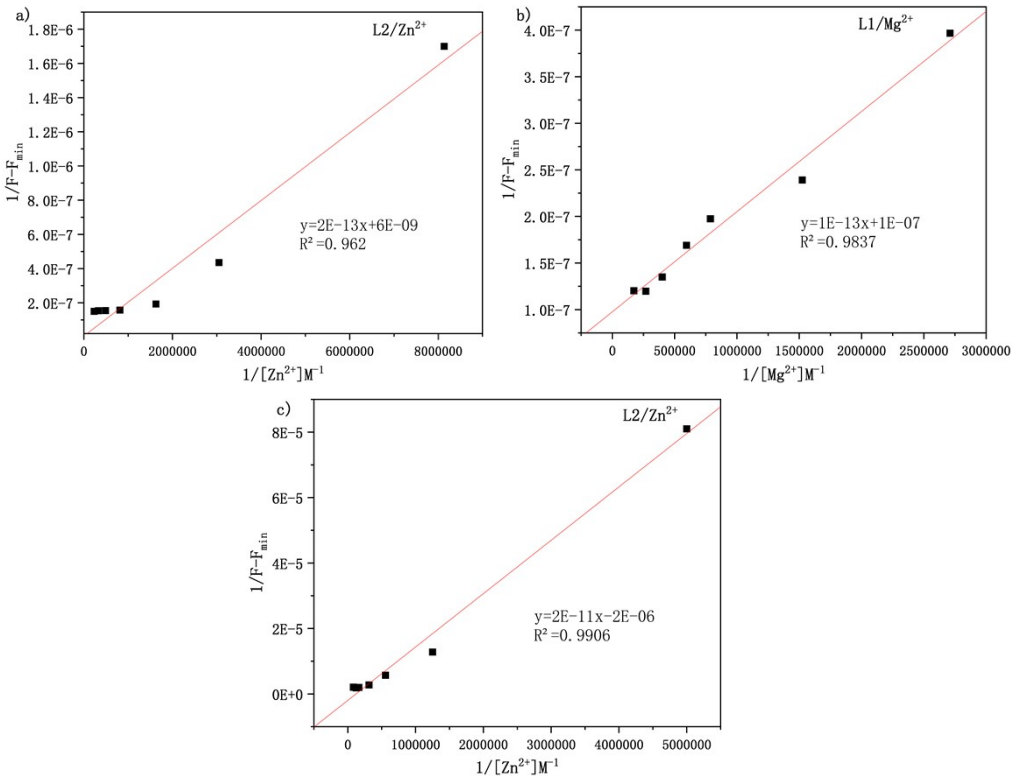

Figure S11. Benesi-Hildebrand curve of the emission changes for the complexation(a) L1/ Zn^{2+}，(b) L1/ Mg^{2+} and (c) L2/ Zn^{2+}.

Table S1.The g_{abs} value of L1/Zn^{2+}， L1/Mg^{2+}

Substance	Corresponding peak(nm)	g_{abs} value
(S,S)-L1	368	1.1129E-03
(R,R)-L1		-1.1124E-03
(S,S)-L1/Zn^{2+}	382	9.7168E-04
(R,R)-L1/Zn^{2+}		-9.4900E-04
(S,S)-L1/Mg^{2+}	377	1.1810E-03
(R,R)-L1/Mg^{2+}		-1.2202E-03
(S,S)-L2	345	2.0230E-03
(R,R)-L2		-2.1840E-03
(S,S)-L2/Zn^{2+}	345	2.4360E-03
(R,R)-L2/Zn^{2+}		-2.4740E-03

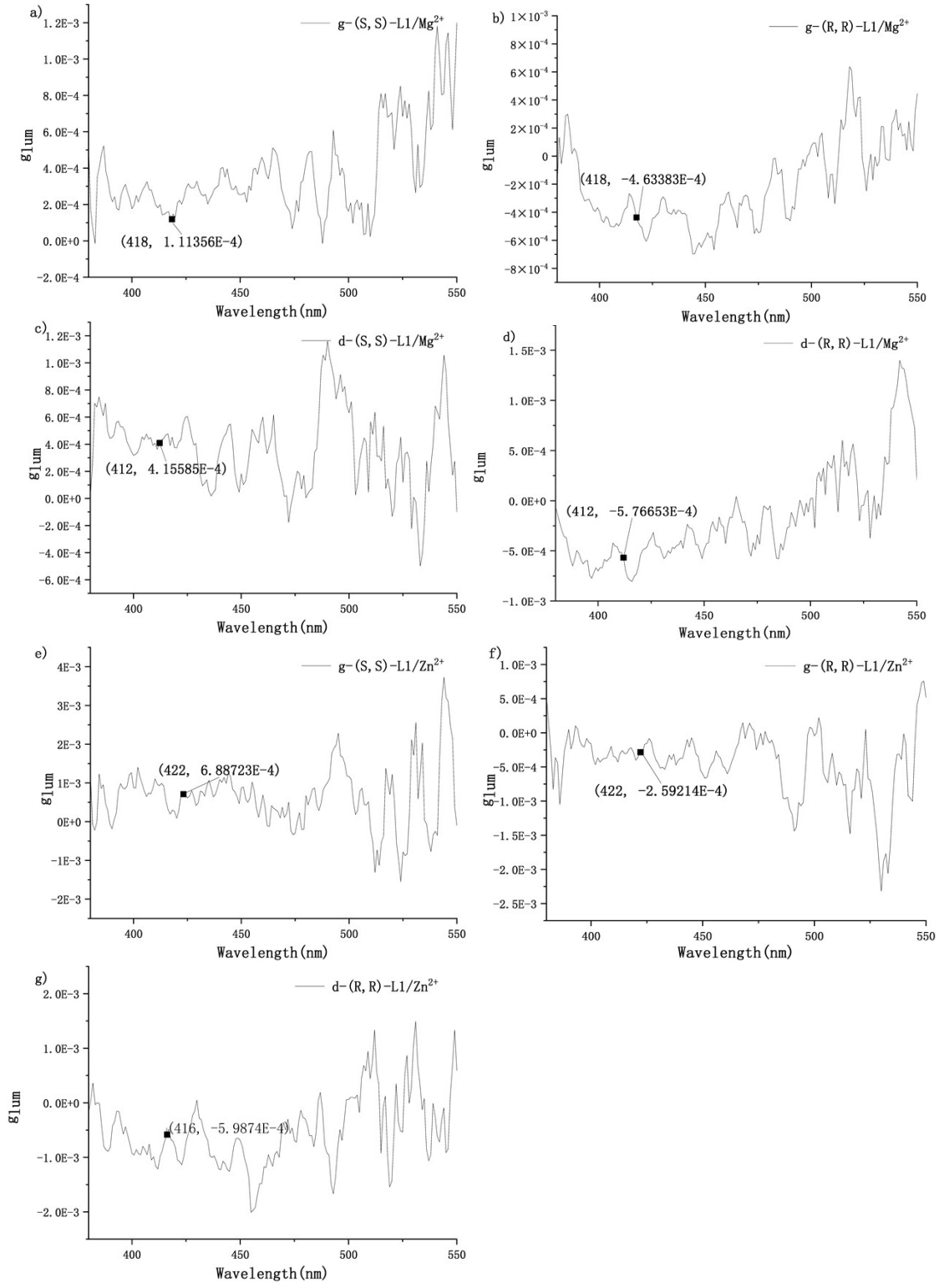

Figure S12. g_{lum} spectra of (a-d) (S,S)/(R,R)-L1/Mg^{2+} and (e-f) (S,S)/(R,R)-L1/Zn^{2+} at two order of magnitude concentration states of 10^{-5} and 10^{-4}. "g" indicates concentration of $3x10^{-4}$ M, "d" indicates concentration of $2x10^{-5}$ M, $Ex_{(CPL)}$=318 nm .

Table S2.The g_{lum} value of L1/Zn^{2+}， L1/Mg^{2+}

Substance	the highest peak in synchronization (nm)	g_{lum} value
(a)g-(S,S)-L1/Mg^{2+}	418	1.11356×10^{-4}
(b)g-(R,R)-L1/Mg^{2+}		-4.63661×10^{-4}
(c)d-(S,S)-L1/Mg^{2+}	412	4.15585×10^{-4}
(d)d-(R,R)-L1/Mg^{2+}		-5.76653×10^{-4}
(e)g-(S,S)-L1/Zn^{2+}	422	6.88723×10^{-4}
(f)g-(R,R)-L1/Zn^{2+}		-2.59214×10^{-4}
d-(S,S)-L1/Zn^{2+}	416	-
(g)d-(R,R)-L1/Zn^{2+}		-5.9874×10^{-4}

IR spectra and DFT Optimized structure calculated

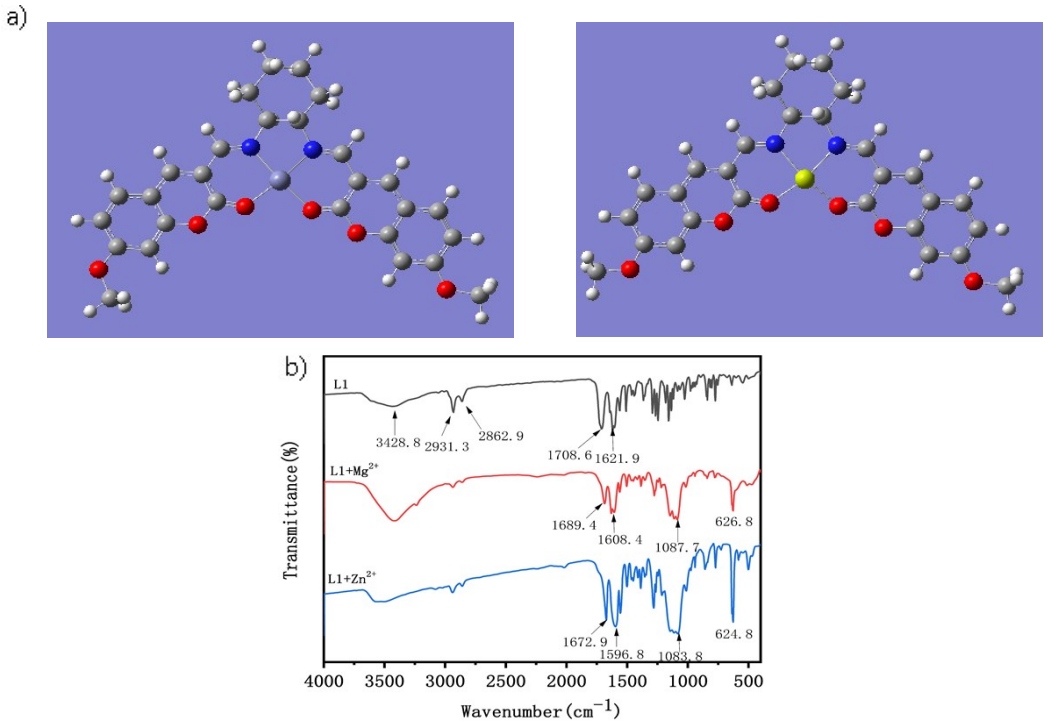

Figure S13. (a) optimized structure calculated at the DFT-B3LYP 6-311g for L1/Zn^{2+} (left)and L1/Mg^{2+}(right);

(b) IR spectra of L1, L1/Zn^{2+} and L1/Mg^{2+}.

Chiral enantiomer recognition FL Spectra of L1 and L2

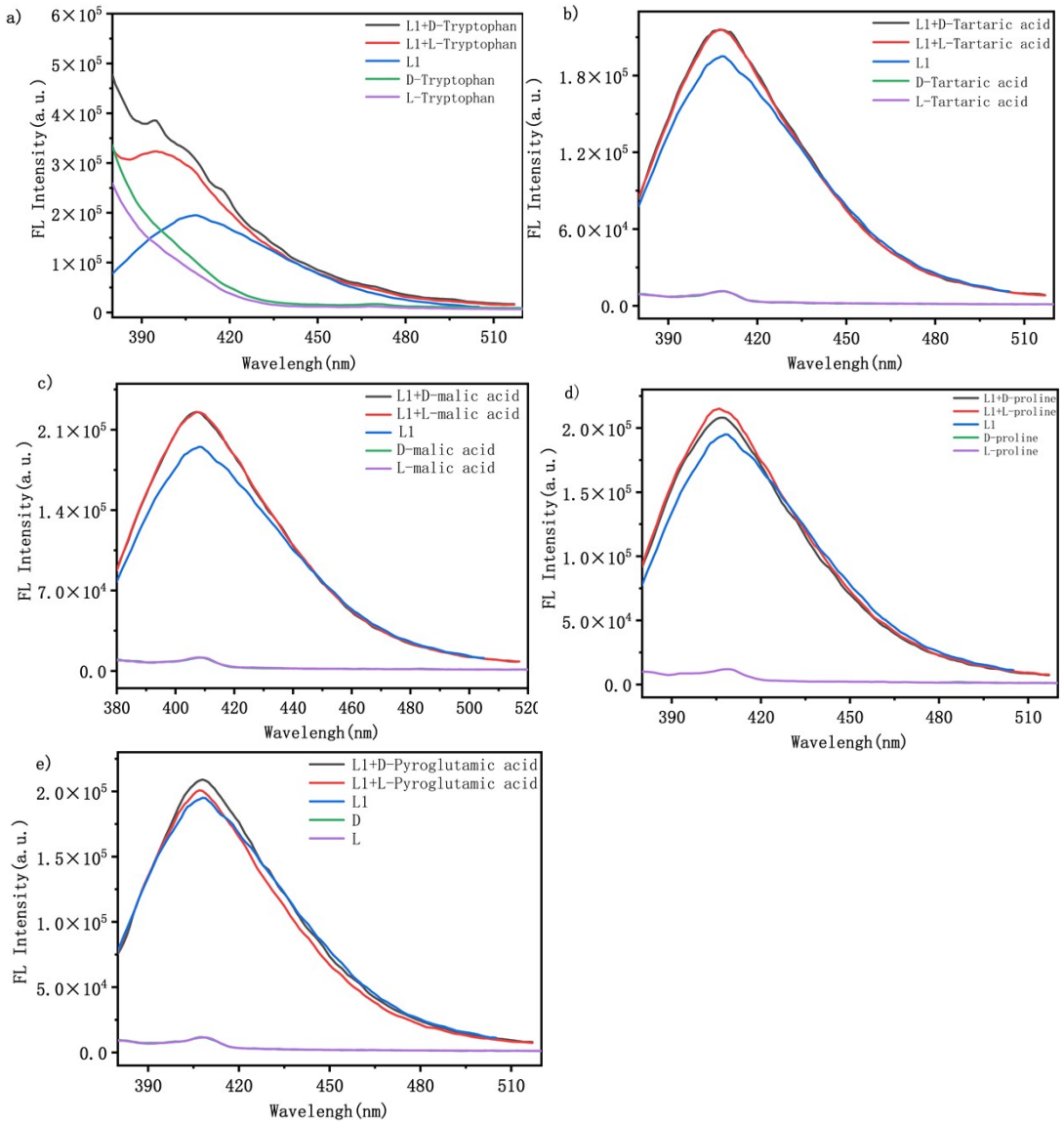

Figure S14. Fluorescence emission spectra of seven chiral enantiomers added to the probe L1 separately (λex=365nm,λem=408 nm; Slit width: EX=5 nm, EM=5 nm). (a): (D)- and (L)-tryptophan; (b): (D)- and (L)-tartaric acid; (c): (D)- and (L)-malic acid; (d): (D)- and (L)-proline; (e): (D)- and (L)-pyroglutamic acid.

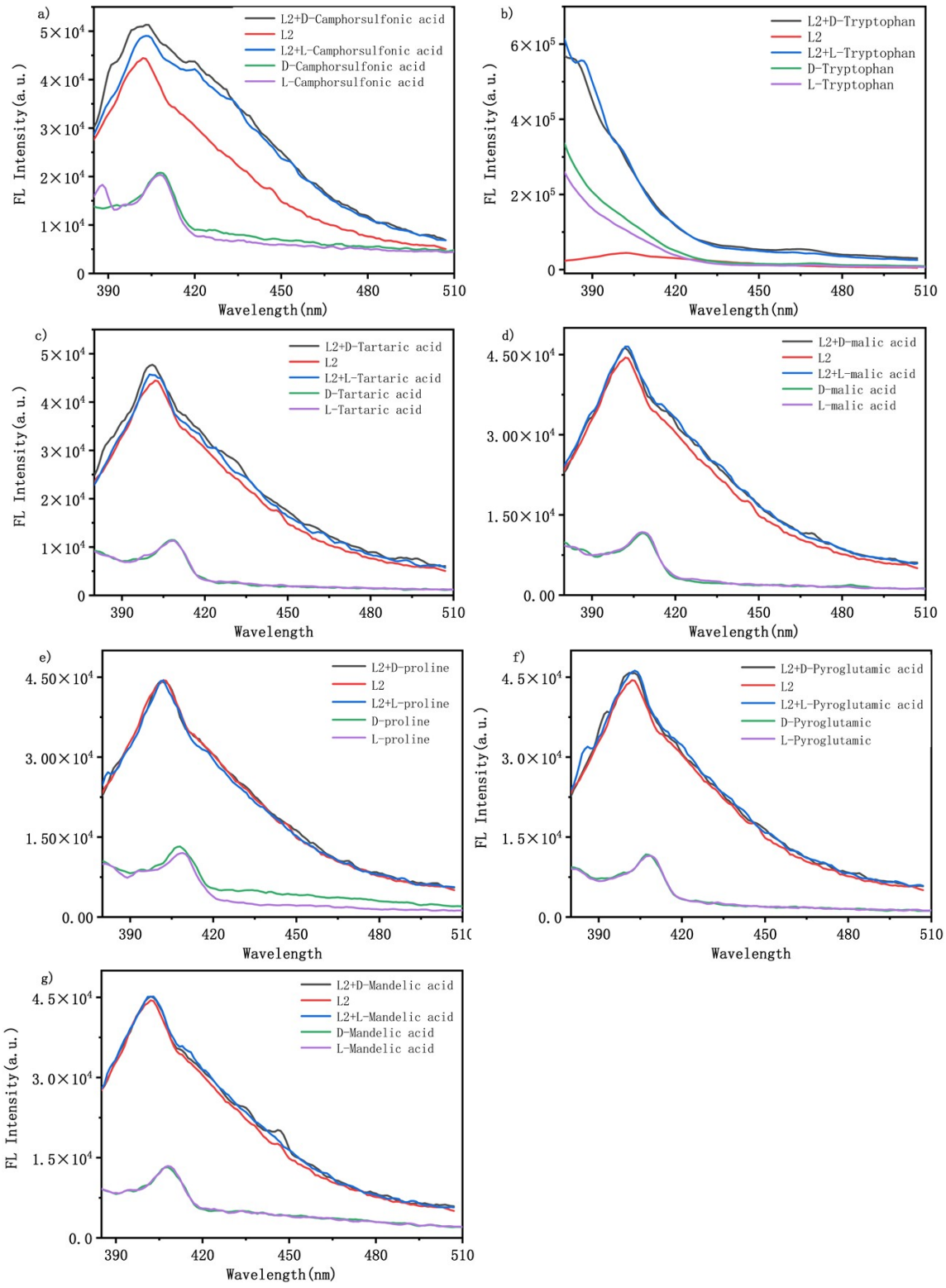

Figure S15. Fluorescence emission spectra of seven chiral enantiomers added to the probe L2 separately (λex=365nm,λem=408 nm; Slit width: EX=5 nm, EM=5 nm). (a): (D)-and (L)-camphorsulfonic acid; (b): (D)- and (L)-tryptophan; (c): (D)- and (L)-tartaric acid; (d): (D)- and (L)-malic acid; (e): (D)- and (L)-proline; (f): (D)- and (L)-pyroglutamic acid; (g): (D) - and (L)-mandelic acid.